

## Outage Contours and Cell Size Distributions in Cellular and Microcellular Networks

Brendan C. Jones, *Student Member, IEEE*, and David J. Skellern, *Member, IEEE*

Electronics Department, School of Maths, Physics, Computing and Electronics  
Macquarie University NSW 2109 Australia

email: brendan@mpce.mq.edu.au, daves@mpce.mq.edu.au

**Abstract:** This paper describes an interference model that provides a simplified description of cellular and microcellular outage contours. The model and computer simulations indicate that cell size variation increases as microcellular systems become more interference limited. Some current cellular and microcellular systems are modelled.

### I. INTRODUCTION

In the design of conventional cellular networks, it is usually assumed that each cell (base station communication region) is a regular shape (circle or hexagon), and that each cell uses a pre-determined set of frequencies (Fixed Channel Allocation or FCA) [1]. This regular cell and frequency plan leads to a simple relationship between the cluster size  $C$  and the signal/interference (S/I) performance of a mobile terminal at a cell boundary in the presence of a cochannel interferer [1].

Current and future microcellular systems, however, usually have no fixed cell geometry and generally use Dynamic Channel Allocation (DCA) and/or transmitter power control to control interference. This enables competing network operators to serve the one geographical area without necessarily conforming to a frequency or base station site plan. As a result, the microcells often overlap and become irregular in shape [2].

The wide scale deployment of an extensive, high grade, wireless telephone system will require engineering tools and techniques that allow rapid and accurate system design [3]. However, there does not yet appear to be a systematic design methodology for engineering a microcellular network to meet a target service quality [3]–[7]. The fundamental problem that needs to be addressed is of modelling the end result of multiple users propagating in a congested area [3],[4].

The applicability of conventional cellular design techniques to the microcellular case is questionable. Firstly, no simple relationship exists between cluster size  $C$  and S/I in microcells [8]. Secondly, consideration of only cochannel interferers may be insufficient, as adjacent and further off-channel interferers can affect the performance of heavily loaded cells [9],[10]. Thirdly, the close spacing of base stations, higher frequency reuse, and spatial traffic variability in microcellular systems have a significant impact upon service quality [2],[5],[7],[11],[12].

### II. INTERFERENCE MODEL

Consider a mobile network consisting of a fixed station  $F_0$  and a mobile station  $M_{00}$  attempting to establish a link in the presence of an arbitrary number  $n$  of fixed stations  $F_i$   $\{1 \leq i \leq n\}$

where each fixed station communicates with an arbitrary number of mobile stations  $M_{ij}$   $\{1 \leq i \leq n, 1 \leq j \leq m_i\}$  where  $m_i$  is the total number of mobile stations communicating with fixed station  $F_i$ . Each mobile station transmits at a power  $P_t$  and is operating on a given channel  $C_{ij}$  and at separations  $r_{ij,0}$  from  $F_0$  as shown in Fig. 1.

The spill power  $P_{ij}$  of each interferer is the radiated power spilled by that interferer into the wanted channel  $C_{ij}$  due to intermodulation products and finite transmitter filter roll-off. Noise in the receivers is considered as a constant interference source with a mean power of  $N$ . At a receiver, a link will be successful ('closes') if the signal to noise plus interference ratio  $S/[N+I]$  is greater than or equal to the system protection ratio  $Z$ .

Extending the approach of [13], consider a single interferer  $F_i$  at a range  $r_{i,0}$  which spills power  $P_u$  into the wanted uplink and  $P_d$  into the wanted downlink. For tractability, a simple distance-dependent path loss propagation model  $P_{rx} = \kappa P_{tx} d^{-\gamma}$  will be used, where  $\kappa$  is a frequency related factor. It can be shown [14] the wanted link closes at the fixed end of the link within a range  $r_{00,0}$  of  $F_0$  if:

$$r_{00,0}^\gamma = \frac{P_t}{ZP_u} \left[ r_{i,0}^\gamma \left( 1 + \frac{N}{\kappa P_u r_{i,0}^{-\gamma}} \right)^{-1} \right] \quad (1)$$

and at the mobile end of the link within a range  $r_{00,0}$  of  $F_0$  if:

$$r_{00,0}^\gamma = \frac{P_t}{ZP_d} \left[ r_{i,0}^\gamma \left( 1 + \frac{N}{\kappa P_d r_{i,0}^{-\gamma}} \right)^{-1} \right] \quad (2)$$

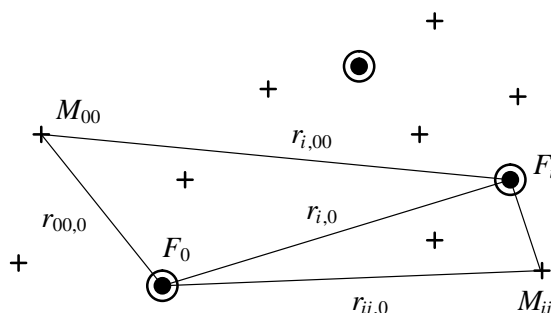


Fig. 1 – Arbitrary mobile network

The term  $N/\kappa P r^{-\gamma}$  is simply the ratio of the noise power to the interference power at the receiver and thus describes the extent of noise or interference dominance of the wanted link. Inverting this ratio and calling it the ‘interference to noise ratio’ or INR, and giving it the symbol  $\eta$ , the above equations may be rewritten respectively as [14]:

$$r_{00,0F}^{\gamma} = \psi \left[ \frac{1}{\eta_F + 1} \right] \quad (3)$$

$$r_{00,0M}^{\gamma} = \psi \left[ \frac{1}{\eta_M + 1} \right] \quad (4)$$

where  $\psi = \kappa P_t / ZN$ ,  $\eta_F = \kappa P_u r_{i,0}^{-\gamma} / N$  and  $\eta_M = \kappa P_d r_{i,00}^{-\gamma} / N$ . As  $\eta_F$  is independent of  $r_{00,0}$  and  $r_{i,0}$  is a constant (3) describes a circle centred on  $F_0$ . However,  $\eta_M$  is not independent of  $r_{00,0}$  and (4) describes a higher plane curve. These two curves are the ‘outage’ curves at each end of a mobile link in the presence of a single interferer. For convenience, the equation for the mobile end outage contour can also be written in terms of  $\eta_F$  using the relationship  $\eta_M = \eta_F (P_d / P_u) (r_{i,0} / r_{i,00})^{\gamma}$ .

The INR describes the extent of interference or noise domination of the wanted link. When  $\eta < 0.1$ , a link is beginning to be noise dominated and when  $\eta > 10.0$  a link is beginning to be interference dominated.

Figs. 2 and 3 show the family of outage contours for  $\eta_F = 0.1$  and  $\eta_F = 10.0$  when  $\gamma = 2$ . The outage contours are marked with their corresponding value of the parameter  $K$ , a relative interference measure, defined as  $K_u = P_t / ZP_u$  for the uplink and  $K_d = P_t / ZP_d$  for the downlink [14]. When  $K = K_e$  the interferer becomes completely enclosed by the mobile end outage contour, and when  $K = K_c$  the mobile and fixed end outage contours intersect at a single point. Expressions for  $K_e$  and  $K_c$  were given in [14].

If it is considered that both ends of the wanted link must close in order to form a satisfactory link, the resultant cell achieved by the mobile terminal  $M_{00}$  is the area of intersection between the mobile and fixed end outage contours. This also means that (3) describes the *maximum* possible range of the mobile terminal regardless of link conditions at the mobile end, and further, when  $K \geq K_c$  the outer cell periphery is determined solely by link conditions at the fixed end.

Examining figs. 2 and 3 it is clear that the resultant cells change greatly in size and shape depending not only upon the relative strength of the interferer (i.e.  $K$ ) but also the INR. In a noise dominated environment (fig. 2) the cells are close to circular except in the immediate vicinity of the interferer. However, in an interference dominated environment (fig. 3) the cell can depart greatly from being circular.

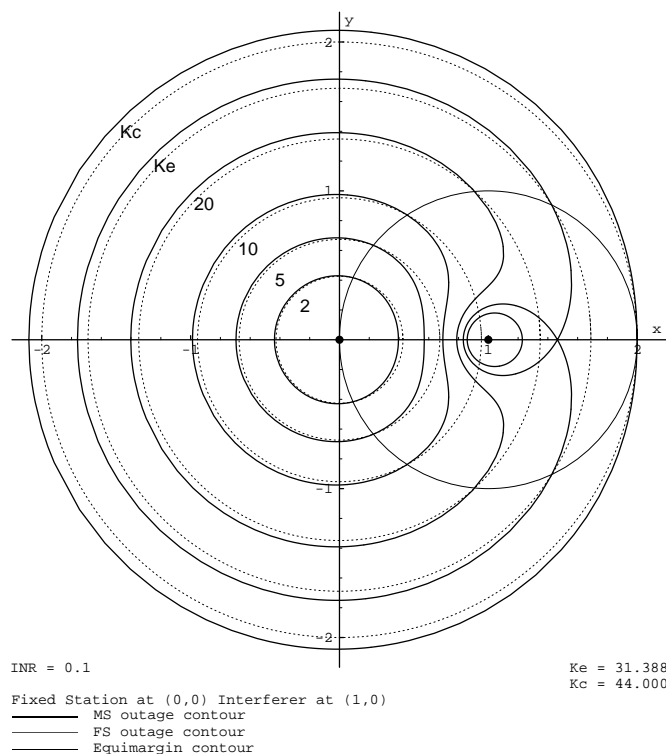


Fig. 2 – Mobile link outage contours versus  $K$  for  $\eta_F = 0.1$  and  $\gamma = 2$

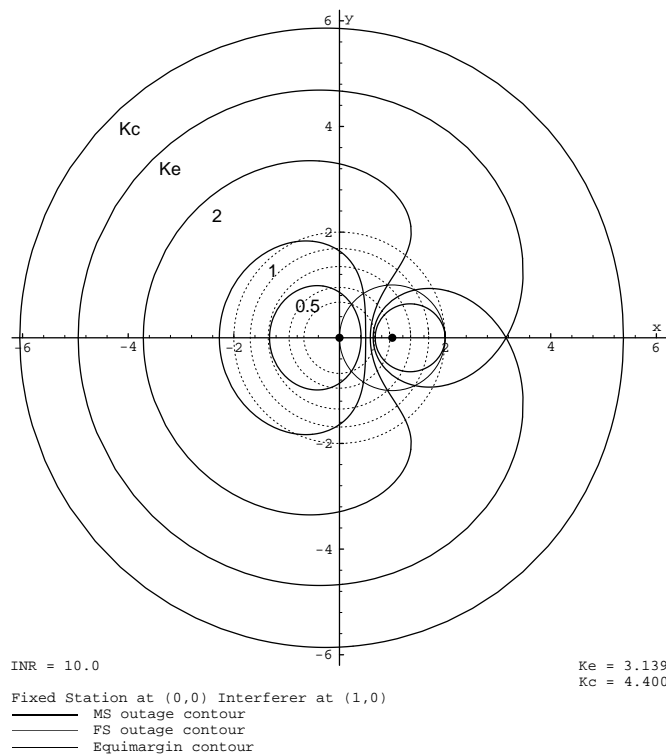


Fig. 3 – Mobile link outage contours versus  $K$  for  $\eta_F = 10.0$  and  $\gamma = 2$

### III. GENERAL OUTAGE CONTOURS

Microcellular networks intend to serve high user densities, and hence each user terminal will potentially operate in the presence of interference from a large number of other users. Under high density conditions, the cumulative interference from *all* users may be significant. Following the interference model described in Fig. 1, the total interference power spilling into the wanted link becomes a summation of individual spill powers from all transmitters, fixed and mobile. Hence the general forms of the INR become:

$$\eta_F = \frac{1}{N} \left\{ \sum_{i=1}^n \left[ \sum_{j=1}^{m_i} [\kappa_{ij} P_{FFij}] r_{i,0}^{-\gamma} \right] + \sum_{i=0}^n \left[ \sum_{j=1}^{m_i} [\kappa_{ij} P_{MFij}] r_{ij,0}^{-\gamma} \right] \right\} \quad (5)$$

$$\eta_M = \frac{1}{N} \left\{ \sum_{i=0}^n \left[ \sum_{j=1}^{m_i} [\kappa_{ij} P_{FMij}] r_{i,00}^{-\gamma} \right] + \sum_{i=0}^n \left[ \sum_{j=1}^{m_i} [\kappa_{ij} P_{MMij}] r_{ij,00}^{-\gamma} \right] \right\} \quad (6)$$

where the subscripts *FF* refers to fixed to fixed station channel spill, *MF* mobile to fixed station channel spill, etc. These equations include channel spill from all users, not just adjacent or cochannel spill. Adjacent channel interference (ACI) is rarely considered in conventional cellular systems, although [15] shows that it can have a significant effect under fully loaded cell conditions with poorly selected channel sets. In contrast, adjacent channel interference is often included in microcellular studies [10],[16],[17]. This model includes all channel spills.

The mobile link outage contours can be shown to be still described by (3) and (4) with  $\eta_F$  and  $\eta_M$  as above. Hence, the fixed end outage contour remains a circle, but the shape of the mobile end outage contour becomes intractable without knowledge of the exact location and channel occupancy of all users. However, as explained in the previous section, (3) describes the maximum possible range of a mobile terminal. In a noise limited system,  $1/(\eta_F+1) \approx 1$  and hence cell sizes will be relatively stable. But as a system becomes more and more interference limited  $1/(\eta_F+1) \approx 1/\eta_F$  and thus cell sizes becomes sensitive to  $\eta_F$  and the arrangement of the interferers.

As microcellular networks have no fixed cell plan, interferers may appear quite close to a wanted link, especially under high usage conditions. Dynamic channel assignment and transmitter power control reduce the probability that interferers will appear close to the wanted link, but it does not make that probability zero, especially in a multioperator environment [5]. Thus

microcellular networks may have a tendency towards interference domination.

Also, each receiver in a cellular or microcellular system will not experience the same level of interference. There may be a wide range of reception conditions, even on links on the one base station, giving rise to some statistical variation of  $\eta$  for receivers in the system. Equations (3) and (4) indicate any such variation will have an increasing impact on the cell sizes achievable (and hence probability of contiguous coverage) as a system becomes more interference limited.

The statistics of  $\eta$  in a system will be a complex function of the location, number and operating channels of all users as indicated by the form of (5) and (6). In practice, the statistics will also be time-varying as users move. As the specific location of other users will be unknown in practice, the effect of increasing cell size variability in interference limited systems may present difficulties in engineering a microcellular network to provide a target grade of service.

### IV. SIMULATION OF CURRENT SYSTEMS

A computer model has been developed to numerically model arbitrary microcellular networks and to test the analytical theory. The model can generate 'snapshot' cell coverage plots or perform Monte Carlo simulations and estimate call blocking and dropout statistics as well as statistical information on the distribution of the interference to noise ratio  $\eta$  for large or complex cellular and microcellular networks.

Fig. 4 shows a snapshot cell coverage plot for one particular mobile station 'under test' ( $\eta_F = 2.1$ ) in a 30 user CT2 system with 5 fixed stations in an irregular arrangement. The black region of the plot indicates where the mobile station would not be able to establish a successful link. The lighter region of the plot indicates where the wanted link can be successfully established with the mobile end of the link having the poorer  $S/[N+I]$ . The darker region of the plot indicates where the wanted link can be successfully established with the fixed end of the link having the poorer  $S/[N+I]$ . It can be seen that the cell periphery is circular in accordance with (3) where the fixed end reception conditions determine the cell extent, and that it is a complicated curve in accordance with (4) where the mobile end reception conditions determine the cell extent.

Cell plots for other mobile stations communicating with the same base station as in Fig. 4 show a wide variation in the size and shape of the cells achieved in accordance with their respective values of  $\eta_F$ . Fig. 5 is but one example, where the mobile station is experiencing a higher level of interference ( $\eta_F = 11.8$ ) and thus experiencing a correspondingly smaller cell.

As indicated earlier, the cell size and shape are a function of the statistics of  $\eta$  which in turn are a complex function of the technical specifications of the cellular technology, user density, and user distribution. An exact analytical approach may not be tractable, so the program can also perform a Monte Carlo simulation to estimate the statistics of  $\eta$  in arbitrary FDMA/TDMA/FDD/TDD cellular or microcellular systems and estimate cell size, call loss and other statistics.

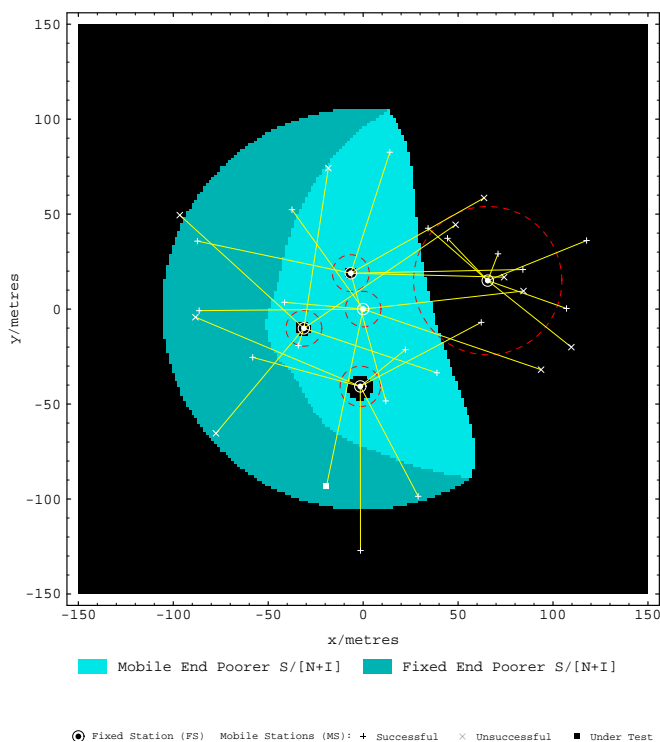


Fig. 4 – Cell coverage for a mobile station in a CT2 system.  
 $\eta_F = 2.1, \gamma = 3.5$

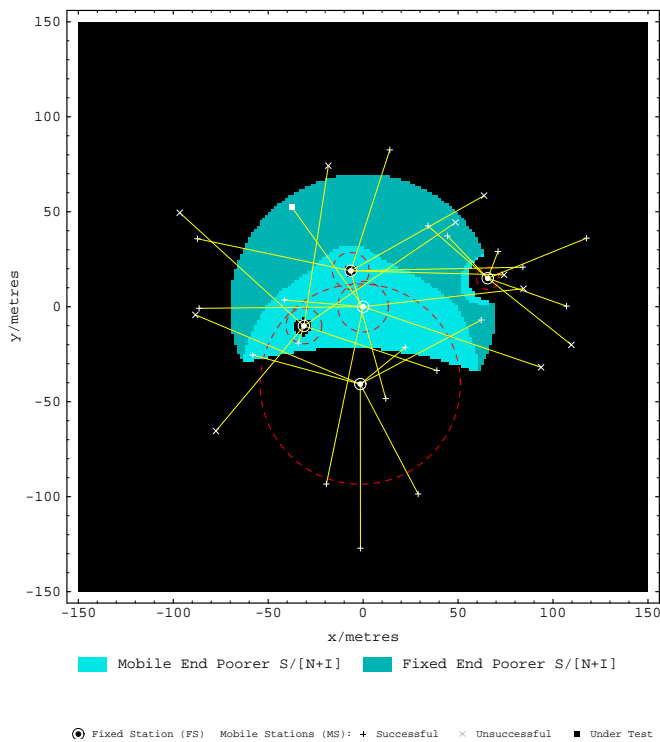


Fig. 5 – Cell coverage for another mobile station in a CT2 system.  
 $\eta_F = 11.8, \gamma = 3.5$

The simulation was loaded with the technical specifications for existing cellular (AMPS and GSM) and microcellular (CT2 and DECT) systems and the call set up and channel allocation procedures used in each. The program generated the statistics of  $\eta_F$  for all *successful* calls when each system was loaded with users to 10% of its channel capacity with a regular central cluster of cells and one tier of surrounding clusters. The propagation exponent  $\gamma$  was set to 3 for both signal and interference. The cluster sizes  $C$  used were 7 for AMPS, 4 for GSM and 1 for CT2 and DECT (i.e. all channels are available in every cell in CT2 and DECT systems).

In each simulation, approximately 10000 call attempts were made. Each round of call attempts consisted of a random sequence of call attempts from mobile stations with the target user loading as indicated in Table I. Mobile stations were placed in random locations for each call attempt but with a uniform distribution in the target service area. A mobile station's call attempt would fail if it didn't meet the required  $S/[N+I]$  at both ends. An initially successful mobile station could also drop out if the success of other mobiles led to an increase in interference, causing its  $S/[N+I]$  to fall below threshold. For DECT and CT2, channel reassignments and retries were allowed in accordance with their specifications. Table I gives a summary of the call failure statistics and  $\eta_F$  statistics. All calls were cleared after each round of call attempts.

The simulation results in Table I suggest that microcellular systems tend towards interference domination (i.e. large values of  $\eta_F$ ) whilst larger cell systems do not, even under high loads and small base station separation. Furthermore, the variation seen in the interference to noise ratio  $\eta_F$  was greater for microcellular systems than in cellular systems as indicated by the increasing standard deviation of  $\log \eta_F$ .

Fig. 6 provides a better view of this distribution by plotting the cumulative distribution statistics (CDF) of  $\eta_F$  on a lognormal scale for the successful calls in each simulation. The dashed lines represent the lognormal lines of best fit to each data, with the slope being inversely proportional to the standard deviation. Fig. 7 shows the cell radius CDF computed from the  $\eta_F$  CDF by using (3).

TABLE I  
 SIMULATION RESULTS FOR SOME MOBILE AND CORDLESS TECHNOLOGIES

PARAMETER	AMPS $C=7$ $P=0.8W$	GSM $C=4$ $P=0.8W$	CT2 $C=1$ $P=0.01W$	DECT $C=1$ $P=0.16W$
Loading (users/cell)	12	25	4	12
Call Blocking (%)	13.31	9.55	1.93	0.53
Call Dropout (%)	8.69	0.32	1.06	0.18
Total Call Loss (%)	22.00	9.88	2.98	0.70
Logarithmic Avg $\eta_F$	0.259	0.333	5.559	9.893
Std Deviation $\log \eta_F$	0.536	0.733	0.762	1.366
Target Cell Radius (m)	1000	1000	100	100
Avg Cell Radius (m)	993.8	1849.4	179.7	319.7

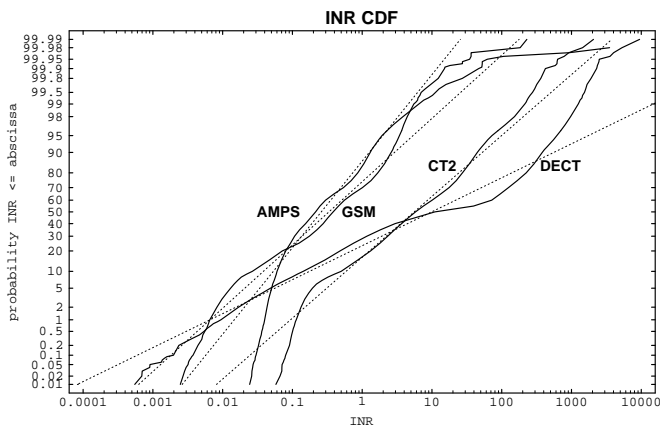


Fig. 6 –  $\eta_F$  CDF for four mobile systems from computer simulation

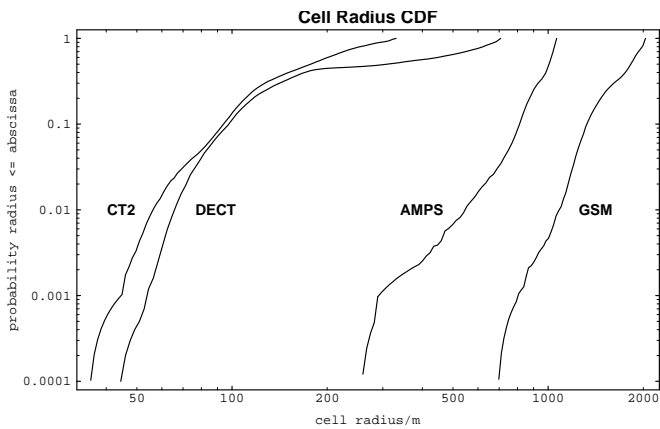


Fig. 7 – Cell radius CDF for four mobile systems from computer simulation

The larger spread of cell sizes clearly evident for the microcellular networks suggests that many mobile terminals may experience much smaller cells than the target radius specified by the fixed station separation, leading to significant coverage gaps and the potential for call loss when the mobile terminals move.

## V. CONCLUSION

Cell sizes experienced by individual mobile stations in a cellular system have been shown to be a function of the “interference to noise ratio” or INR at that mobile’s fixed station. The shape of the outage contour is also a function of the INR.

Simulations have shown that the INR has a higher average value in the microcell systems modelled than in similarly loaded large cell systems, indicating that the microcell systems modelled tend towards interference domination. This effect, coupled with the larger deviation in the INR in the microcell systems modelled, resulted in microcells having a larger variation in cell sizes than large cell systems.

These results suggest that a system wide microcellular design methodology will need to address the statistics of the INR in a

system if contiguous coverage is required for a certain proportion of mobile stations. The quality of the cell coverage may also impact upon the overall Quality of Service. Further development of the analysis approach described in this paper is expected to form the basis for a systematic microcellular engineering methodology.

## REFERENCES

- [1] W.C.Y. Lee, *Mobile Communications Design Fundamentals*, 2nd ed., John Wiley and Sons, New York, 1993.
- [2] D. Everitt and D. Manfield, “Performance analysis of cellular mobile communication systems with dynamic channel assignment”, *IEEE J. Sel. Areas Comm.*, vol 7 no 8, pp 1172–1180, Oct 1989.
- [3] T.S. Rappaport, “Wireless personal communications: Trends and challenges”, *IEEE Ant. Prop. Mag.*, vol 33 no 5, pp 19–29, Oct 1991.
- [4] J. Sarnecki, C. Vinodrai, A. Javed, P. O’Kelly and K. Dick, “Microcell design principles”, *IEEE Comm. Mag.*, vol 31 no 4, pp 76–82, Apr 1993.
- [5] P.A. Ramsdale, A.D. Hadden and P.S. Gaskell, “DCS1800 – The standard for PCN”, *6th IEE Int. Conf. Mobile and Personal Comm.*, pp 175–179, Coventry, UK, 9–11 Dec 1991.
- [6] I. Goetz, “Transmission planning for mobile telecommunications systems”, *6th IEE Int. Conf. on Mobile Radio and Personal Comm.*, pp 126–130, Coventry, UK, 9–11 Dec 1991.
- [7] A.O. Fajokuju, A. McGirr and S. Kazeminejad, “A simulation study of speech traffic capacity in digital cordless telecommunications systems”, *IEEE Trans. Veh. Tech.*, vol 41 no 1, pp 6–16, Feb 1992.
- [8] W.T. Webb, “Modulation methods for PCNs”, *IEEE Comm. Mag.*, vol 30 no 12, pp 90–95, Dec 1992.
- [9] S.S. Rappaport and S.-W. Wang, “Signal to interference calculations for balanced channel assignment patterns in cellular communications systems”, *IEEE Trans. Com.*, vol 37 no 10, pp 1077–1087, Oct 1989.
- [10] J.P. Driscoll, “Relevance of receiver filter performance and operating range for CT2/CAI Telepoint systems”, *Electron. Lett.*, vol 28 no 13, pp 1200–1201, 18 Jun 1992.
- [11] D.C. Cox, “Wireless network access for personal communications”, *IEEE Comm. Mag.*, pp 96–115, Dec 1992.
- [12] S. Sato, K. Takeo, M. Nishino, Y. Amezawa, T. Suzuki: “A performance analysis on nonuniform traffic in microcell systems”, *IEEE Int. Conf. on Comm. (ICC 93)*, vol 3, pp 1960–1964, Geneva, Switzerland, 23–26 May 1993.
- [13] C.E. Cook, “Modeling interference effects for land–mobile and air–mobile communications”, *IEEE Trans. Com.*, vol 35 no 2, pp 151–165, Feb 1987.
- [14] B.C. Jones and D.J. Skellern, “Interference modelling and outage contours in cellular and microcellular networks”, *2nd MCRC Int. Conf. on Mobile and Personal Comm. Sys.*, Adelaide, Australia, 10–11 April 1995, in press.
- [15] S.S. Rappaport and S.-W. Wang, “Signal to interference calculations for corner excited cellular communications systems”, *IEEE Trans. Com.*, vol 39 no 12, pp 1886–1895, Dec 1991.
- [16] J.E. Button, “Asynchronous CT2/CAI Telepoint separation requirements”, *Electron. Lett.*, vol 27 no 1, pp 48–49, 3 Jan 1991.
- [17] Y.-D. Yao and A.U.H. Sheikh, “Performance analysis of microcellular mobile radio systems with shadowed cochannel interferers”, *Electron. Lett.*, vol 28 no 9, pp 839–841, 23 Apr 1992.